JOURNAL OF GEOPHYSICAL RESEARCH, VOL. 112, D05309, doi:10.1029/2006JD007632, 2007

Click Here for Full Article

Trans-Pacific transport of black carbon and fine aerosols ($D < 2.5$ μm) into North America

O. L. Hadley,[1] V. Ramanathan,[1] G. R. Carmichael,[2] Y. Tang,[2,3] C. E. Corrigan,[1] G. C. Roberts,[1] and G. S. Mauger[1]

Received 7 June 2006; revised 26 September 2006; accepted 8 December 2006; published 14 March 2007.

[1] This study presents estimates of long-range transport of black carbon (BC) and aerosol fine mass (diameter less than 2.5 μm) across the Pacific Ocean into North America during April 2004. These transport estimates are based on simulations by the Chemical Weather Forecast System (CFORS) model and evaluated across 130°W, (30°N–60°N) from 26 March through 25 April 2004. CFORS calculates BC transport into North America at 25–32 Gg of which over 75% originates from Asia. Modeled fine aerosol mass transport is between 900 and 1100 Gg. The BC transport amounts to about 77% of the published estimates of North American BC emissions. Approximately 78% of the BC and 82% of the fine aerosol mass transport occur in the midtroposphere above 2 km. Given the relatively large magnitude of the estimated BC transport, we undertake a detailed validation of the model simulations of fine aerosol mass and BC over the west coast of North America. In situ aircraft data were available for the month of April 2004 to assess the accuracy of model simulations of aerosols in the lower troposphere. Aircraft data for aerosol mass collected in the eastern Pacific Ocean during April 2004 as part of the Cloud Indirect Forcing Experiment, as well as surface measurements of fine mass and BC at 30 west coast locations, are compared to CFORS predictions. These surface sites are part of the Interagency Monitoring of Protected Visual Environments (IMPROVE) network. Both the aircraft and the IMPROVE data sets reveal similar patterns of good agreement near and above the boundary layer accompanied by large overprediction within the boundary layer. The observational data validate the CFORS simulations of BC and fine aerosol mass above the boundary layer. The near-surface overprediction does not impair the major conclusions of this study regarding long-range aerosol and BC transport, as most of the long-range transport occurs above 2 km. From this we conclude that the transport of BC from Asia and other regions west is a major source of BC at high elevations over North America. The simulated concentrations of BC between 1 and 3 km, as well as the measured BC concentrations over the elevated IMPROVE sites, range from 0.1 to 0.3 μg/m^3. Direct radiative forcing over North America due to the modeled BC concentration between 1 and 15 km is estimated at an additional 2.04–2.55 W/m^2 absorbed in the atmosphere and a dimming of -1.45 to -1.47 W/m^2 at the surface. The impact of transported BC on the regional radiation budget through direct and indirect effects of the transported BC and other aerosols warrants further study.

Citation: Hadley, O. L., V. Ramanathan, G. R. Carmichael, Y. Tang, C. E. Corrigan, G. C. Roberts, and G. S. Mauger (2007), Trans-Pacific transport of black carbon and fine aerosols ($D < 2.5$ μm) into North America, *J. Geophys. Res.*, *112*, D05309, doi:10.1029/2006JD007632.

1. Introduction

[2] Growing interest in long-range transport of pollutants across the Pacific Ocean has motivated a number of field experiments as well as the development of chemical transport models. Employing both field data and models, several studies have characterized trans-Pacific transport of carbon monoxide and ozone [*Bertschi and Jaffe*, 2005; *Goldstein et al.*, 2004; *Liang et al.*, 2004; *Yienger et al.*, 2000], as well as various other pollutants [*Jacob et al.*, 2003; *Parrish et al.*, 2004]. Observational and modeling analyses have identified

[1]Center for Atmospheric Sciences, Scripps Institution of Oceanography, University of California San Diego, La Jolla, California, USA.
[2]Center for Global and Regional Environmental Research, University of Iowa, Iowa City, Iowa, USA.
[3]Now at National Centers for Environmental Prediction, NOAA, Camp Springs, Maryland, USA.

Copyright 2007 by the American Geophysical Union.
0148-0227/07/2006JD007632$09.00

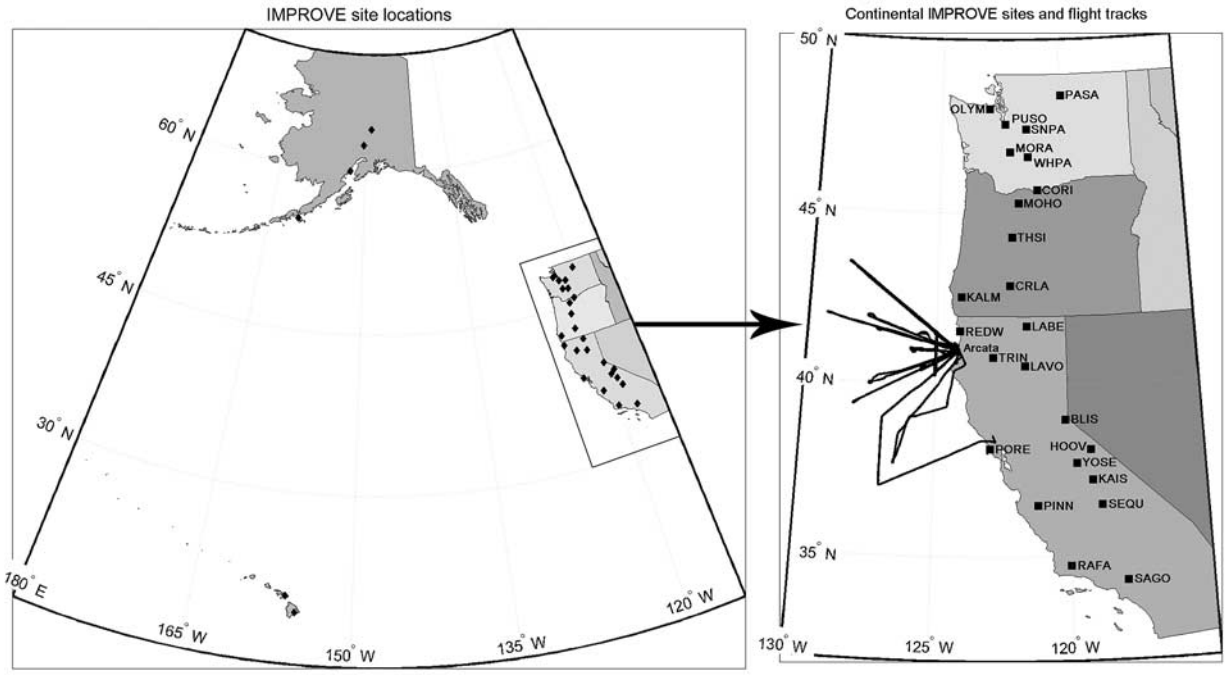

Figure 1. IMPROVE site locations and the WY King Air flight tracks.

episodic and significant enhancement from Asian dust and pollution emissions at a multitude of surface sites in the western United States [*Heald et al.*, 2006; *Jaffe et al.*, 2005; *VanCuren and Cahill*, 2002]. Studies have also shown that continental outflow of Asian pollution [*Bey et al.*, 2001], including black carbon (BC) [*Park et al.*, 2005], is largest during the spring, which is the end of the dry season in Asia when desert dust emissions are at a maximum. A high frequency of vernal cold fronts moving across the northwest Pacific rapidly lifts the prefrontal aerosols and other pollutants to altitudes where they are captured by high winds and carried toward North America [*Jacob et al.*, 2003; *Liu et al.*, 2003; *Stohl*, 2001]. Although spring meteorology enhances Asian aerosol transport, long-term and short-term surface aerosol analyses during the Intercontinental Transport and Chemical Transformation 2002 (ITCT 2K2) field study provide evidence that Asian pollution impacts the northeast Pacific Ocean and the west coast of North America year-round and that background levels of tropospheric aerosol at altitudes greater than 1 km over the western United States are largely of Asian origin [*VanCuren et al.*, 2005]. This paper assesses transport of BC, as well as fine aerosol mass, into North America during April 2004.

[3] The Chemical Weather Forecast System (CFORS) model provided estimates of BC and aerosol mass transport over the Pacific Ocean from 26 March to 25 April 2004. Comparison with aircraft and surface aerosol data validates the model estimates. The aircraft data were collected during Cloud Indirect Forcing Experiment (http://borneo.ucsd.edu/cifex/) (CIFEX), which took place during April 2004 off the coast of northern California. Aerosol and cloud data were collected on board the King Air, a twin turbo-prop aircraft operated by the University of Wyoming, which flew 24 missions [*Roberts et al.*, 2006] from 1–24 April in the region bound by 37°N–43°N and 124°W–127.5°W (Figure 1, right panel). The King Air is equipped with multiple aerosol instruments for tropospheric measurements [Table 1, adapted from *Roberts et al.*, 2006]. This was ideal for CIFEX, which focused on the measurement of aerosol and cloud properties to assess the impact of long-range transport on aerosol-cloud interactions. The experiment operated from the Eureka/Arcata airport in northern California [near the Trinidad Head site operated by the (National Oceanic and Atmospheric Administration-Climate Monitoring and Diagnostics Laboratory, NOAA-CMDL)], where we intercepted plumes of pollution and dust transported from the Asian continent across the Pacific Ocean. A wide variety of aerosols observed included those of long-range transport from Asia, clean marine boundary layer, and North American emissions. These aerosols, classified by their size distribution and history, were found in stratified layers between 500 and 6500 m above sea level and thicknesses from 100 to 3000 m [*Roberts et al.*, 2006]. In addition to the airborne measurements, we employed measurements of elemental carbon (EC), organic carbon (OC), sulfate, and fine dust (<2.5 μm) from various Interagency Monitoring of Protected Visual Environments (IMPROVE) sites in Alaska, Hawaii, Oregon, Washington, and California (Figure 1). The IMPROVE sites sampled varied fractions of Asian air mass ranging from less than 10% for low-elevation sites to an excess of 40% for the higher elevation sites (Table 2).

2. CFORS Model

[4] CFORS couples observed meteorological fields (i.e., reanalysis fields) with surface emissions of pollutants to simulate three-dimensional distribution of pollutant gases and chemical composition of aerosols [*Uno et al.*, 2003]. The trans-Pacific tracer domain extends from 15°N to 80°N and between 110°E and 105°W, with a horizontal resolution

Table 1. Wyoming King Air Instrument Payload During CIFEX, April 2004[a]

Instrument	Measurement	Sample Rate, s
Condensation Particle Counter (CPC 3760; TSI)	Concentration (N_{CN}; $D_p > 10$ nm)	1
Scanning Mobility Particle Sizer (SMPS; TSI)	Size distribution ($n(D_p)$; $10 < D_p < 400$ nm)	50
Passive Cavity Aerosol Spectrometer Probe (PCASP-100X; PMS)	Size distribution ($n(D_p)$; $0.2 < D_p < 3$ μm)	1
Integrating nephelometer (Radiance Research)	Hemispherical scattering (σ_b; $\lambda = 530$ nm)	1
Forward Scattering Spectrometer Probe (FSSP-100; PMS/DMT)	Size distribution ($n_D(D_p)$; $1 < D_p < 45$ μm)	1

[a]Adapted from *Roberts et al.* [2006].

of 200 km. Vertical resolution of the CFORS atmosphere is given in 18 layers ranging in thickness from 50 m at the surface to over 1000 m at the top altitude of 15 km. Output variables include concentrations of BC, sulfate, fine dust, and OC, the sum of which we use as a measure of total aerosol mass. The model incorporates wet and dry removal parameters for dust, sulfate, OC, and SO_2, as well as first-order oxidation conversion of SO_2 to sulfate [*Uno et al.*, 2003]. A wet removal parameter for BC, equal to that of SO_2, was incorporated during this study [*Uno et al.*, 2003]. In the CFORS model, wet removal affects only the atmospheric layers below cloud base, which is determined from the Regional Atmospheric Modeling System (RAMS) hydrometeor field [*Uno et al.*, 2003].

[5] Spatial distributions of column-integrated concentrations of BC and aerosol fine mass obtained from CFORS are shown in Figure 2 for April 2004. For comparison, Figure 3 shows aerosol visible optical depth (AOD) for April 2001 and 2004 obtained from Moderate Resolution Imaging Spectroradiometer [MODIS; *Tanre et al.*, 1997]. Figures 2 and 3 reveal similar patterns of large values in eastern China with the pollution plume extending in the northeastern direction toward North America. Eastward transport of dust, anthropogenic sulfur dioxide, and sulfate across 130°E between 15°N and 75°N (Figure 2, solid white line at 130°E) was calculated from CFORS output and compared with analogous CFORS calculations made during ACE-Asia (Table 3), April 2001 [*Seinfeld et al.*, 2004]. Modeled daily average transport of dust and sulfate across 130°E between 26 March and 25 April 2004 equals only a third of the CFORS estimates for April 2001 (Table 3). MODIS retrievals of AOD for April 2001 and 2004 (Figure 3) also show reduced AOD for 2004 in the eastern Pacific, thereby corroborating the reduced transport estimated by CFORS for 2004 compared to 2001.

[6] For the CIFEX campaign, CFORS used *Streets et al.* [2003] for Asian emission inventories of sulfate, SO_2, OC, and BC. US EPA inventory for 2001 supplied North American emissions for CFORS calculations. Surface wind speed, soil wetness and texture, and ground cover control surface dust emissions [*Uno et al.*, 2003], and the vertical temperature profile determines the dust uplift height. From 26 March through 25 April, CFORS-derived BC net transport between 30°N and 60°N (Figure 2, solid line) at 130°W was 32 Gg, of which roughly 75% originates from Asian sources. This amounts to 77% of the estimated 41.5 (27–93) Gg of BC emitted monthly from North American sources [*Bond et al.*, 2004]. The CFORS net fine aerosol mass transport for the period of 26 March to 25 April was 1100 Gg. Figure 4 shows the vertical profile of the average 26 March to 25 April CFORS BC, Asian BC, and fine aerosol mass transport at 130°W, between 30°N and 60°N. The temporally and spatially integrated transport between the surface and 2 km is 7 Gg of BC, and the rest, 25 Gg, is transported within the free troposphere above 2 km. For fine aerosol mass, the surface to 2 km layer transports 200 Gg and the region above 2 km sees 900 Gg. Thus the dominant transport (78% of BC and 82% of fine aerosol mass) occurs above 2 km.

[7] The accuracy of CFORS fine mass and BC transport is assessed next by considering the following observed properties: (1) the vertical distribution of fine mass in the eastern Pacific Ocean taken from aircraft data between 200 and 6500 m and (2) surface concentrations of EC, OC, SO_4, and fine dust at elevations ranging from 15 to 2700 m.

3. Vertical Profiles of Aerosol Mass Concentration From Aircraft

[8] Out of the 24 research flights, 8 provided data on the vertical and horizontal aerosol number distribution in the eastern Pacific within a 400-km range of Trinidad Head, CA. These eight flights were chosen because they provide both vertical aerosol profiles, as well as level flights of significant length that were free of cloud contamination. The remaining 16 flights were primarily dedicated to cloud analysis. The flight tracks are shown in Figure 1 (right panel). These data include vertical aerosol profiles between

Table 2. IMPROVE Sites: Location and Percentage of Air Mass Trajectories Originating from Asia

Site	Latitude	Longitude	Elevation	% Asian Trajectories
BLIS CA	39	−120.1	2130.7	55
CORI WA	45.7	−121	178.5	5
CRLA OR	42.9	−122.1	1996	40
DENA AK	63.7	−149	658.2	0
HALE HW	20.8	−156.3	1153	25
HAVO HW	19.4	−155.3	1258.5	25
HOOV CA	38.1	−119.2	2560.7	45
KAIS CA	37.2	−119.2	2597.5	55
KALM OR	42.6	−124.1	80	15
LABE CA	41.7	−121.5	1459.5	30
LAVO CA	40.5	−121.6	1732.7	40
MOHO OR	45.3	−121.8	1531	20
MORA WA	46.8	−122.1	439	10
OLYM WA	48	−123	599.7	20
PASA WA	48.4	−119.9	1627.3	25
PINN CA	36.5	−121.2	302	5
PORE CA	38.1	−122.9	97	15
PUSO WA	47.6	−122.3	97.7	0
RAFA CA	34.7	−120	956.5	10
REDW CA	41.6	−124.1	243.7	20
SAGO CA	34.3	−118	1791	35
SEQU CA	36.5	−118.8	519.3	0
SIME AK	55.3	−160.5	57	10
SNPA WA	47.4	−121.4	1049	30
THSI OR	44.3	−122	885	15
TRCR AK	62.3	−150.3	155	0
TRIN CA	40.8	−122.8	1014	35
TUXE AK	60	−152.7	15	0
WHPA WA	46.6	−121.4	1827.3	45
YOSE CA	37.7	−119.7	1603	45

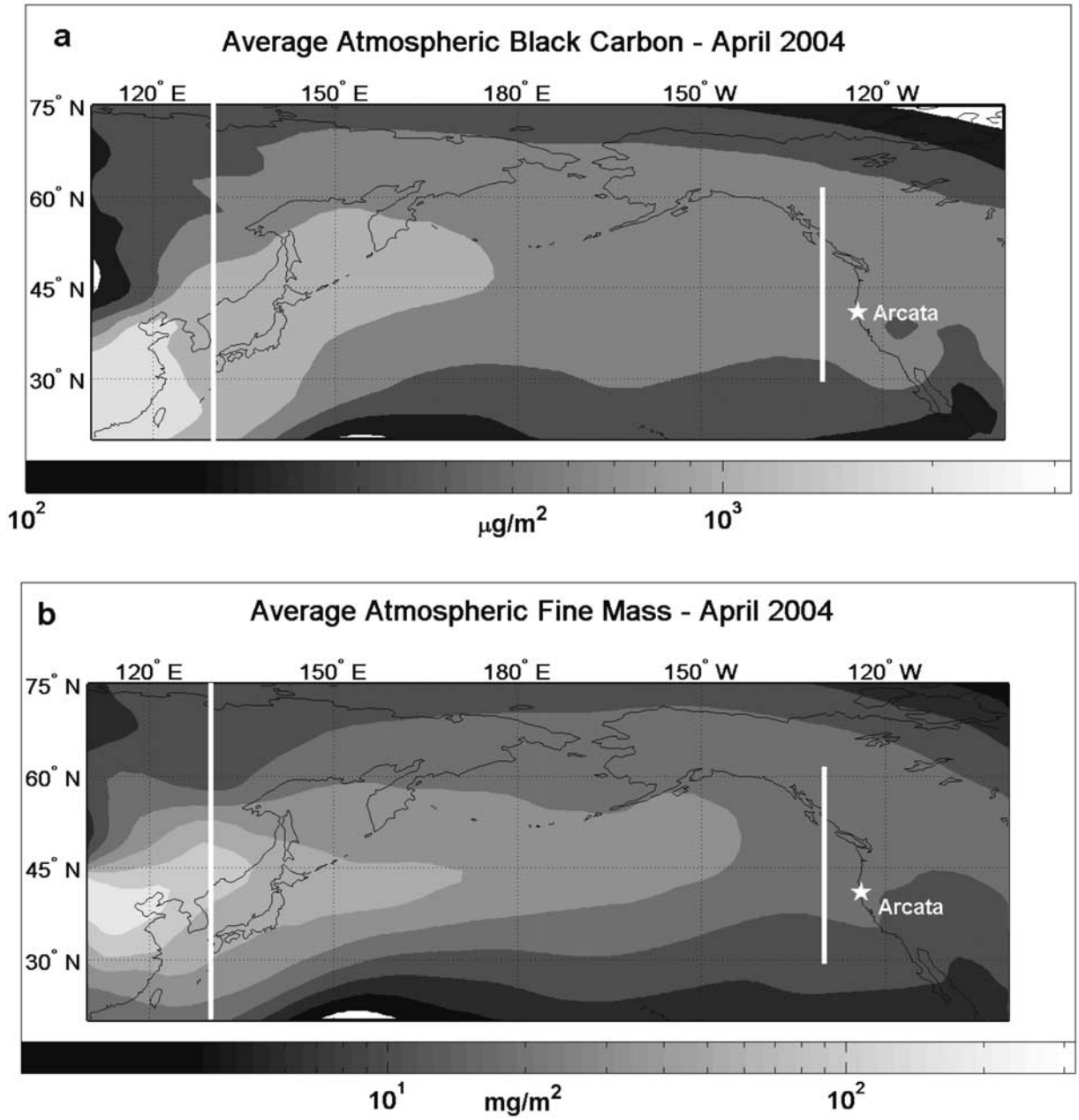

Figure 2. CFORS-derived atmospheric column (a) BC and (b) fine mass, averaged from 26 March to 26 April 2004. White lines indicate the latitude range where transports were calculated in Table 3.

200- and 6500-m (max altitude of the King Air) level, clear-sky, flight legs at varying altitudes, each lasting between 6 and 30 min.

[9] Aerosol size distributions were obtained with a Scanning Mobility Particle Sizer (SMPS) for particles between 0.013- and 0.3-μm diameter, and a Passive Cavity Aerosol Spectrometer probe (PCASP) for particles between 0.1- and 2.5-μm diameter. The PCASP was calibrated to a refractive index of 1.58, and PCASP sizes were corrected assuming a refractive index of 1.45 [*Stolzenburg et al.*, 1998]. Diameter corrections were obtained from *Liu and Daum* [2000]. Combining the SMPS and PCASP spectra produced approximately one aerosol size spectrum per minute for diameters ranging from 0.01 to 2.5 μm. There is a 10% (±12%) discrepancy between integrated spectra and mean condensation particle counter (CPC) concentrations for the same period. Mass concentration was calculated using an aerosol density of 1.9 g cm^{-3}. Uncertainty estimates were calculated from the one sigma standard deviation of number concentration in each size bin and an uncertainty in aerosol density of ±30% [*Wittmaack*, 2002]. The total uncertainty in calculated aerosol mass is ±31%. CFORS fine mass is defined as the sum of fine dust, sulfate, OC, and BC mass concentration. Validation for this assumption is provided in section 4. The CFORS output includes the minimum and maximum aerosol mass concentration forecast by the model 12 hours prior and 12 hours following flight times as a measure of temporal sampling variability.

[10] Vertically integrated aerosol mass obtained from the data taken during the eight clear-sky flight days agrees

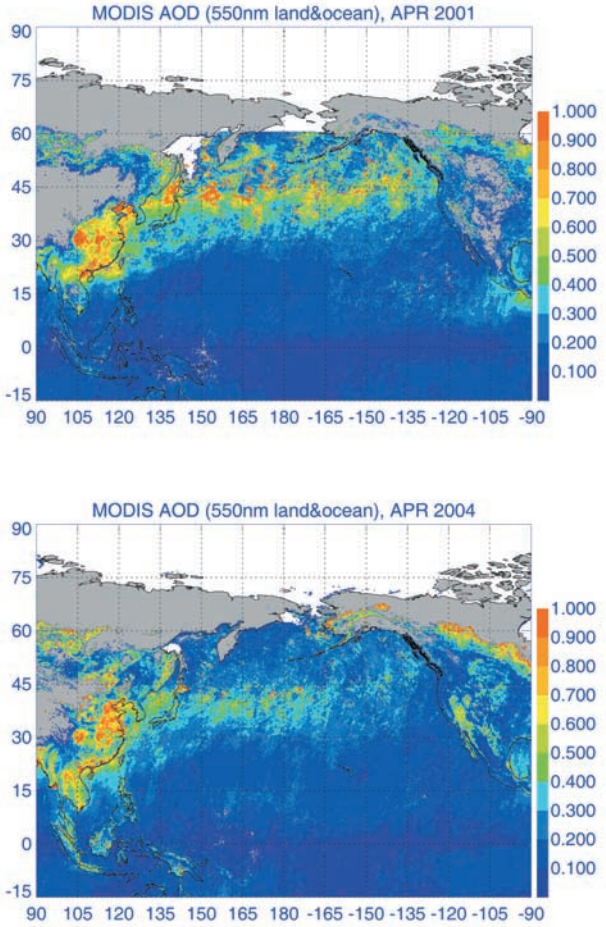

Figure 3. MODIS retrievals of average AOD in April 2001 and April 2004.

with the CFORS prediction for the middle troposphere (2–5.5 km) within 3% (Figure 5a); however Figure 5b indicates that CFORS overpredicts the fine mass in the lower troposphere (0–2 km) by 280% (±140%). The mean, April 2004, aerosol mass vertical distribution, representing all level flights and vertical profiles collectively, compares similarly to the averaged April 2004 CFORS vertical mass distribution (Figure 6). CFORS predictions agree well with flight data above the boundary layer but overpredict aerosol mass near the surface 140–420%.

4. Comparison of CFORS With IMPROVE Network Data

[11] IMPROVE network sites supplied BC and fine mass (<2.5-μm diameter) aerosol data for 28 March through 24 April 2004 at 30 sites in Alaska, Washington, Oregon, California, and Hawaii (Figure 1). This study compares these data to the CFORS model outputs at each IMPROVE site location. Elevations of the IMPROVE sites range from 15 to 2600 m. Only CFORS outputs coincident with the time of IMPROVE sampling were used in the comparison.

[12] The IMPROVE network provided bulk fine aerosol mass concentration, as well as chemical composition by mass. Desert Research Institute conducted all the filter analyses and supplied the IMPROVE data used in this report. Fine mass was obtained from gravimetric measurements. The thermal optical reflectance method was used to retrieve EC and OC mass values [*Chow et al.*, 2004]. One caveat to this method is that the values reported for OC and EC assume that all CO_2 evolved at temperatures less than 550°C in the absence of O_2 is due to organics, and all CO_2 evolved before the filter reflectance returns to the initial value. If these assumptions are incorrect, then the given OC may be 30% higher than the actual amount, and likewise the EC could be underpredicted. Soil (μg m^{-3}) is calculated using [*Eldred et al.*, 1997]:

$$\text{Soil} = 2.20 \times \text{Al} + 2.49 \times \text{Si} + 1.63 \times \text{Ca} + 2.42 \times \text{Fe} + 1.94 \times \text{Ti}. \quad (1)$$

[13] Ion chromatography is used to determine the sulfate concentration collected on fine nylon filters [*Eldred and Cahill*, 1997].

[14] In this study, the IMPROVE fine mass is calculated as the sum of the PM2.5 soil, sulfate, BC, and OC mass concentration. This corresponds to the components summed in the CFORS model to represent total fine mass. On average, these four species account for 70% (±10%) of the bulk, fine aerosol mass measured at each site. Other aerosol components not included in the model output and likely contributing to the observed mass are nitrates, sea salt, and the noncarbon fraction of organic mass.

[15] Figure 7 compares the April 2004 average, vertical distribution of the CFORS output, and the IMPROVE data for (a) the fine aerosol mass concentration and (b) the average BC mass concentration during the CIFEX campaign. The EC IMPROVE data are used as observed BC, and IMPROVE soil data represent the observed fine dust. As with the CIFEX flight data comparisons, CFORS generally overpredicts the fine mass at low altitudes and is in closer agreement with the IMPROVE data at higher elevations. The average percent difference of fine mass above 1000 m is 47% compared with 155% for the lower elevations. Analogous to the fine mass comparisons, CFORS overpredicts the IMPROVE BC below 1000 m on average by 214%, whereas above 1000 m, the average percent difference between model and observations is 18%.

[16] For both BC and fine mass, the largest differences between observations and the CFORS model occur below

Table 3. CFORS-Modeled Anthropogenic Sulfate, SO_2, Dust, and BC Transport During CIFEX 2004 and ACE-Asia 2001

Aerosol	ACE-Asia 130E, 5–15 April 2001 [*Seinfeld et al.*, 2001]	CIFEX—130E, 26 March to 25 April 2004	CIFEX—130W 26 March to 25 April 2004
Sulfate (Gg/day)	36	11	9
SO_2 (Gg/day)	-	13	1
Dust (Tg/day)	1.27	0.42	0.06

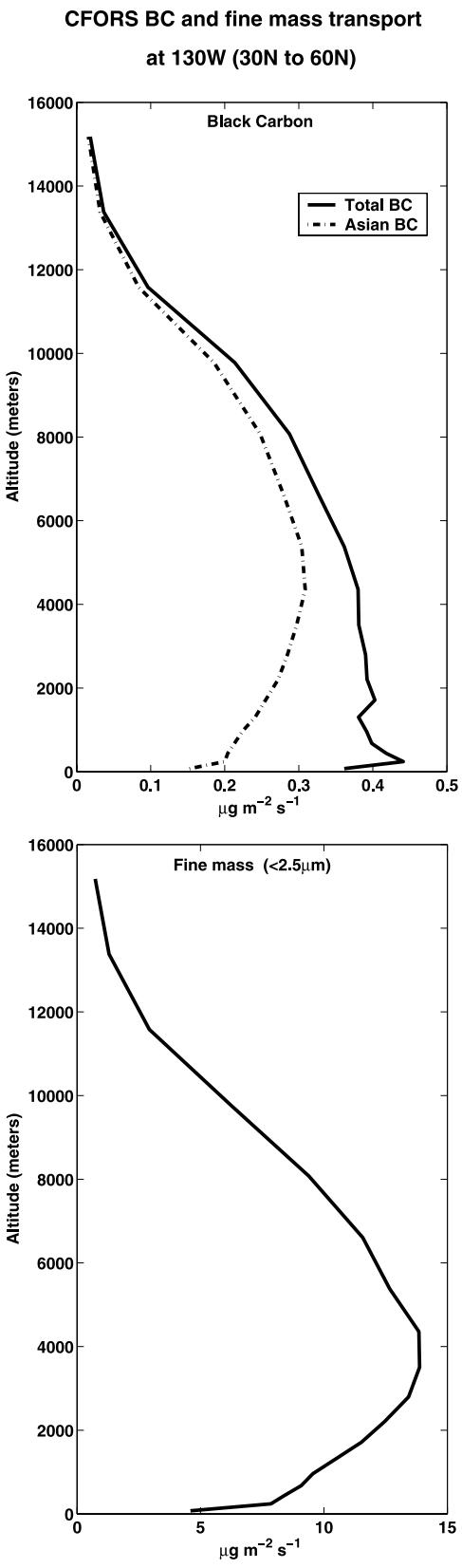

Figure 4. Average total BC, Asian BC, and fine mass transport across 130°W (between 30°N and 60°N) from 26 March to 25 April relative to altitude.

1000 m and decrease with increasing altitude. The comparison between CFORS and the IMPROVE data, shown as a function of altitude, is consistent with the CIFEX flight data presented in Figures 5 and 6, which show similar results in the altitude ranges of the IMPROVE sites. The best agreement between model and flight observation is above 2.5 km.

[17] Figure 8 presents the IMPROVE and CFORS comparison for each of the remaining aerosol components individually: (a) fine dust/soil, (b) OC, and (c) sulfate. These data clearly demonstrate that the largest discrepancy between model and observations lies in the fine dust prediction, where the only agreement coincides with the two highest elevation sites. Both OC and sulfate appear to be well predicted at all elevations, with exceptions at a few sites. Above 1000 m, the average percent differences for OC, sulfate, and fine dust are −13, 8, and 209, and 107, 21, and 746% below 1000 m.

4.1. Factors Contributing to the Surface Overestimation

[18] Since the boundary layer transport represents a minor fraction of the long-range transport of aerosols, we have not conducted a detailed analysis of the factors contributing to the large overestimation of BC and dust within the boundary layer, but offer the following speculations. CFORS-simulated rainfall points to a potentially major factor contributing to the model deficiency in the near surface layers. Precipitation data, obtained from the NOAA NCEP CPC REGIONAL US_Mexico daily gridded archive http://ingrid.ldeo.columbia.edu/SOURCES/.NOAA/.NCEP/.CPC/.REGIONAL/.US_Mexico/.daily/.gridded/.archive/, provide a means of evaluating the CFORS/RAMS precipitation output for all sites in Washington, Oregon, and California. Results show that CFORS precipitation generally appears in the right place at the right time. Model and observations are correlated with an r^2 equal to 0.53 (Figure 9). However, the model regularly produces rain totals, which on average are only a third of the gridded rain data, and often misses a rain event entirely. A combination of inadequate wet removal parameters and insufficient precipitation throughout transport may help explain the overprediction at low altitudes. *Uno et al.* [2003] found that CFORS tended to overpredict both sulfate and EC during rain events, but that, in general, the model observation agreement at the surface was quite good in the western Pacific Ocean. In addition, errors in North American dust and BC emissions likely contribute to the boundary layer overprediction observed over the west coast of North America. CFORS agreement with observations at higher altitudes compared with those at the surface show that although the model has difficulty forecasting locally generated pollutants and boundary layer processes, the predictions for long-range transport of Asian aerosols and BC at high altitudes are reasonable estimates.

4.2. Asian Tracers and Air Mass Trajectories in CFORS and IMPROVE Data

[19] In the CIFEX flight regions, CFORS estimates that 78% of the BC transport above 2 km comes from Asia (Figure 10), with the remaining aerosol mass originating from the Arctic (including Alaska), north of 60°N, and recirculation from North America, south of 30°N, and Central America. CFORS isolates the Asian BC from the

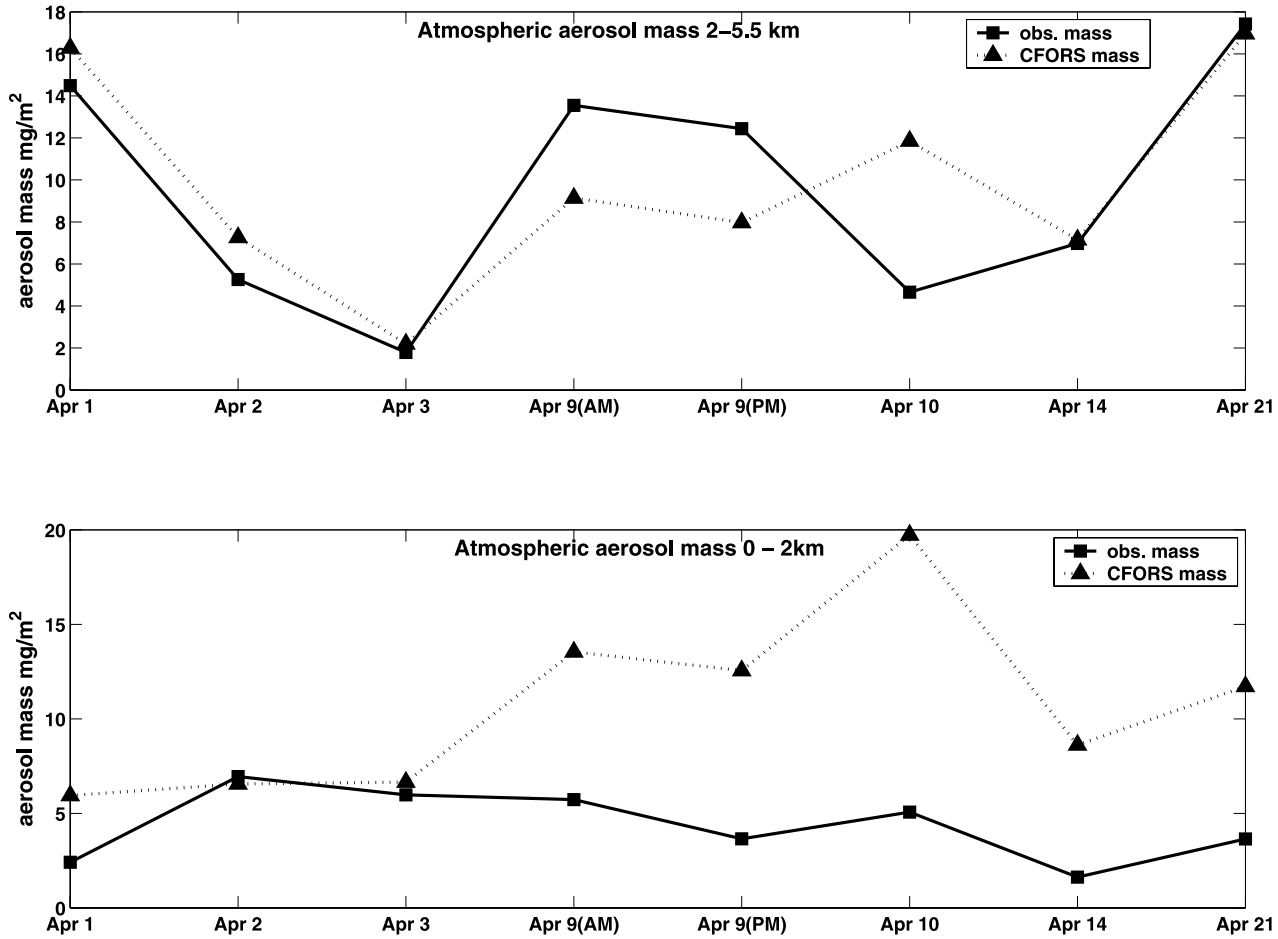

Figure 5. Modeled and calculated aerosol mass: (a) between 2 and 5 km and (b) below 2 km. Aerosol mass was derived from observations of number concentration and size distribution on board the WY King Air.

total BC as a separate variable using only BC emitted from Asian sources. The CFORS Asian BC percentage represents the increasing Asian influence on total aerosol mass with altitude. This is consistent with analysis of the IMPROVE Pb data and the NOAA-HYSPLIT (Hybrid Single-Particle Lagrangian Integrated Trajectory) [*Draxler and Hess*, 1998] 10-day back-trajectories discussed below.

[20] A 4-year time series (2001–2004) of the average Pb-to-fine-mass ratio for both high (>1600 m) and low (<700 m) IMPROVE sites in Washington, Oregon, and California (Figure 11a) displays a significant annual peak during winter and early spring at the high-elevation sites and a reduced signal and ratio at the lower elevations. The 4-year time series of absolute Pb concentration (Figure 11b) indicate prominent peaks in spring and fall for both high-elevation and low-elevation sites; however, the springtime peaks dominate at high elevations. As Asia produces three times more Pb per year than North America [*Pacyna and Pacyna*, 2001] and since both Pb concentrations in Taipei [*Hsu et al.*, 2005] and IMPROVE Pb concentrations in western North America are highest during the period of Asian transport, it makes a useful indicator of Asian influence on the aerosol measured at the IMPROVE sites. The Pb-to-fine-mass ratio from the IMPROVE data correlates significantly, although not strongly, to the CFORS Asian BC fraction. The correlation coefficient is significant at 0.34. The 95% confidence limits are narrow between 0.21 and 0.45, and the probability that they are uncorrelated is 3×10^{-7}. The correlation coefficient for the high-elevation sites increases to $r = 0.4$ (0.16–0.59). The Pb ratio and Asian BC fraction are completely uncorrelated at $r = 0.036$ (−0.18 to 0.25) for sites below 700 m. The correlation between Pb and EC in Hong Kong was found to be between 0.7 and 0.8 [*Zheng and Fang*, 2000]. Due to unique variability of local and Asian Pb and BC emissions, as well as errors in the CFORS boundary layer simulation, it is not surprising that the correlation is not higher. The significance, however, confirms the CFORS-simulated increase in Asian BC fraction with altitude.

[21] In addition to the Pb data, a comparison of the HYSPLIT [*Draxler and Hess*, 1998] air-mass 10-day back-trajectories for a selection of high (>1700 m; Figure 12a) and low (<700 m; Figure 12b) elevation sites, coincident with the IMPROVE aerosol collection days, also indicates a more frequent and pronounced Asian influence on the air masses arriving at high-elevation sites. Air masses arriving at low-elevation sites originate almost entirely from the central Pacific; however, the IMPROVE Pb data

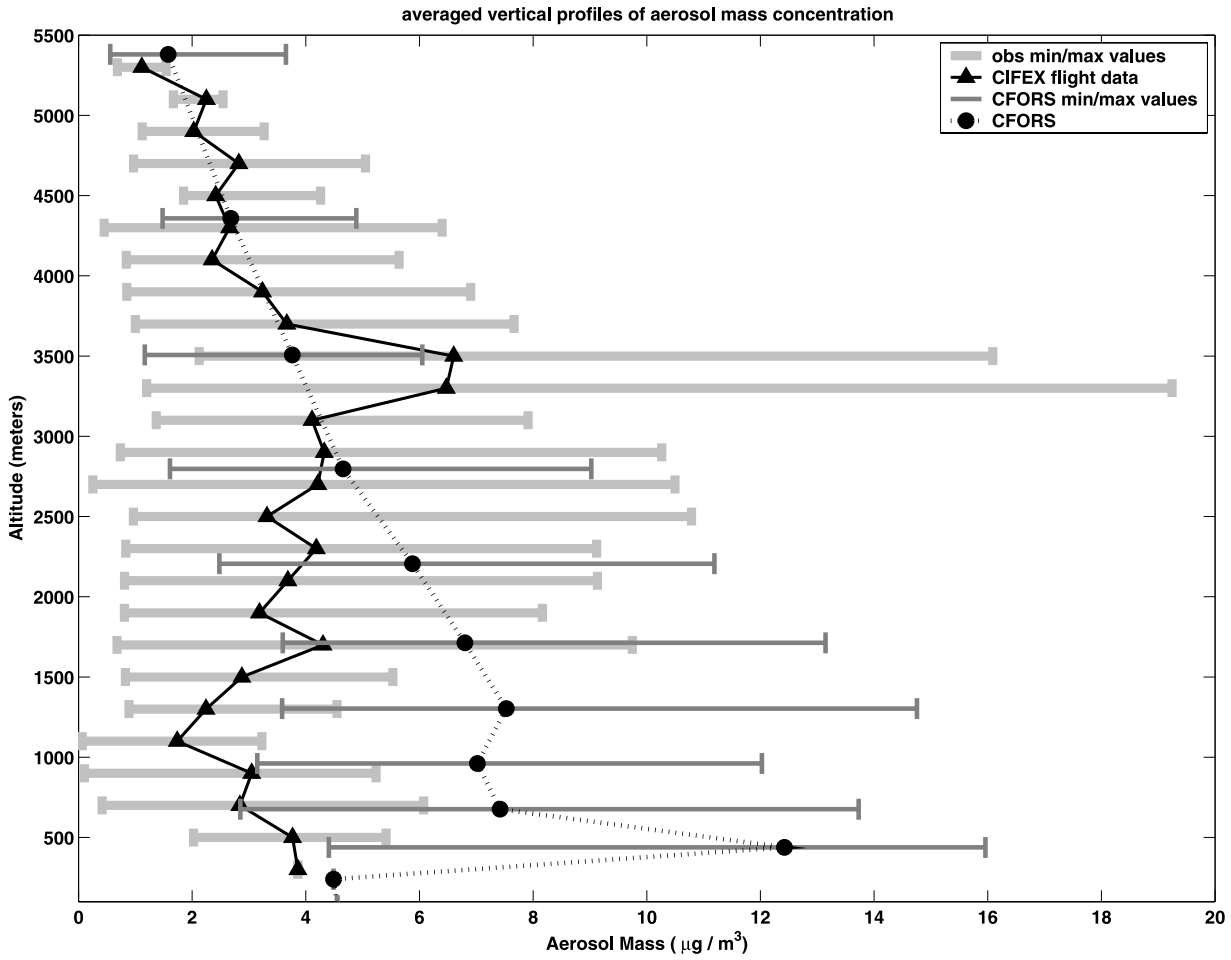

Figure 6. Comparison of vertical distribution of CFORS aerosol mass with derived aerosol mass from CIFEX flights. Minimum and maximum values recorded in each layer are shown as the window of variability for aerosol mass concentration.

(Figure 11a) show a small springtime peak in the Pb-to-PM2.5 ratio for low-elevation sites, suggesting downward mixing from the layers of long-range transport aloft. The low altitudes of the trajectories, combined with the seasonal signal in Pb data at low elevations, point toward significant mixing with marine aerosol for surface air masses. Asian–marine aerosol mixtures were also observed at low-altitude surface sites during ITCT 2K2 [*VanCuren et al.*, 2005]. Observations of enhanced springtime transport of Asian sulfate and dust at high-elevation IMPROVE sites in the NW United States are reported by *Heald et al.* [2006]. The back-trajectories for all sites are consistent with this analysis, showing an increase in the percentage of days when air masses appear to originate in Asia or eastern Europe as elevation increases (Figure 13).

5. Implications to Radiation Budget and Climate

[22] The simulated concentrations of BC between 1 and 3 km, as well as the measured BC concentrations, range from 0.1 to 0.3 μg m^{-3} (Figure 7b). Above 3 km, CFORS BC exponentially decreases with altitude (Figure 14). Because of fast large-scale transport in the free troposphere above the boundary layer, BC and other aerosols can be transported across North America in less than a week. There are several reasons why the transported BC can have important effects in regional radiation budget and climate. First, absorption of solar radiation by BC increases solar heating of the atmosphere and decreases solar radiation at the surface. In cloudy regions, BC in clouds can enhance the absorption and surface dimming (compared to the BC effects in clear skies) significantly if it is internally mixed with the cloud droplets [*Chylek and Hallett*, 1992; *Mikhailov et al.*, 2006]. Since the transported BC has been airborne for several days, it is most likely hydrophilic and hence internally mixed with the droplets [*Mikhailov et al.*, 2006]. Last, BC and dust transported from Asia can impact upper tropospheric clouds over North America through the so-called indirect effect [*Abbatt et al.*, 2006; *Hendricks et al.*, 2005; *Lohmann et al.*, 2004; *Pruppacher and Klett*, 1997]. For example, using ground-based lidar polarization data, *Sassen et al.* [2003] indicated that Asian aerosols influence the formation and phase of ice clouds, leading to anomalously warm cirrus ice clouds. Midtropospheric and upper tropospheric clouds exert a strong greenhouse effect, in addition to increasing the planetary albedo, particularly over the Pacific Ocean where longwave cloud forcing (i.e., greenhouse effect) is between 35 and 50 W/m^2, whereas the shortwave cloud forcing is

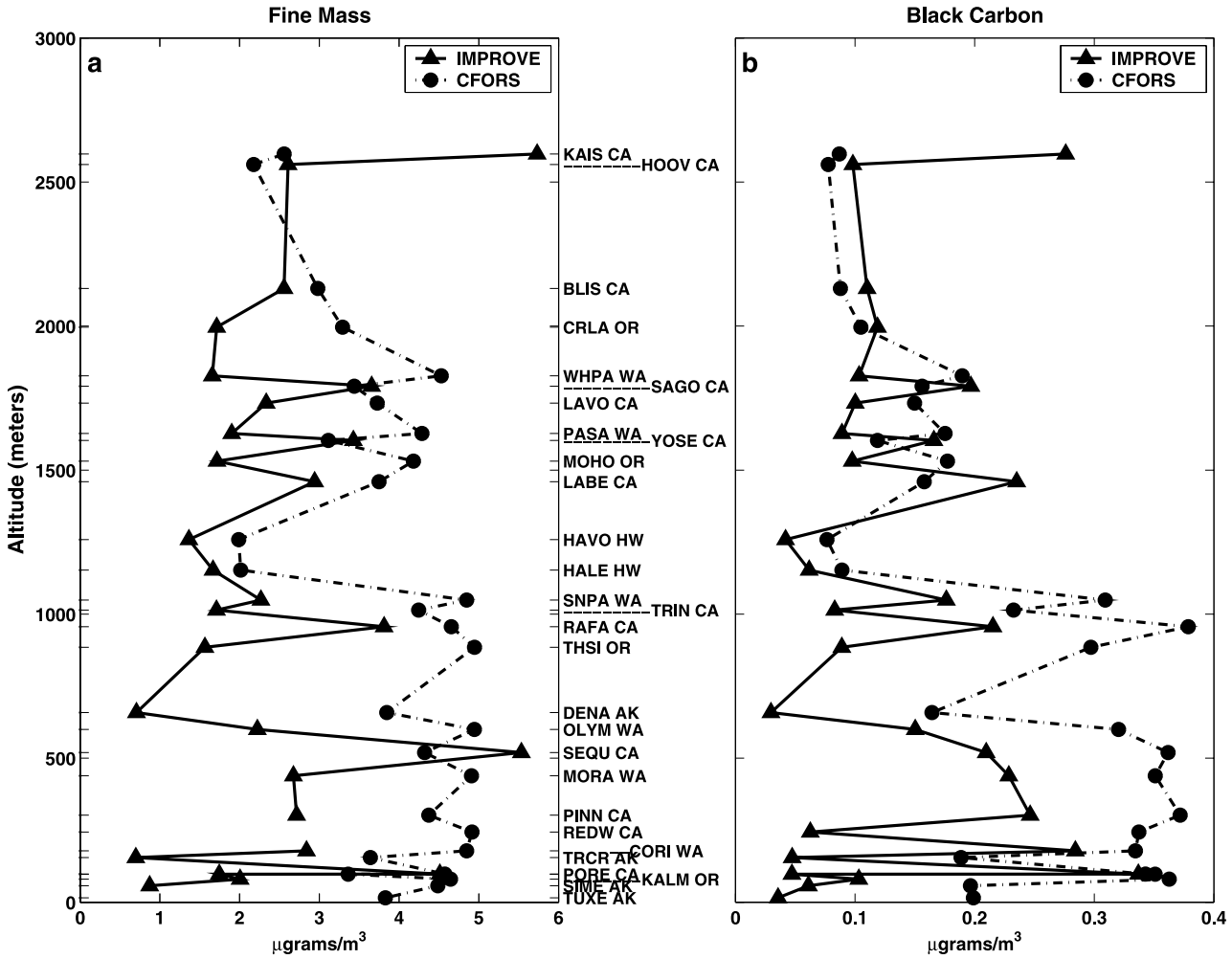

Figure 7. Comparison of vertical distribution of (a) CFORS and IMPROVE fine aerosol mass and (b) CFORS and IMPROVE BC. The IMPROVE fine aerosol represents the soil, organic carbon, elemental carbon, and sulfate contribution to the total aerosol mass, for comparison with the same species comprising the CFORS aerosol mass.

from −60 to −95 W/m^2 [*Ramanathan et al.*, 1989]. Thus a preferential increase in the greenhouse effect of a few watts per square meter (e.g., due to an increase in thin cirrus cloud optical depth or lifetime due to increased ice nuclei) can amplify the greenhouse forcing. On the other hand, if the presence of BC with dust leads to warmer cirrus clouds, the greenhouse effect would be suppressed and the albedo effect would dominate and lead to a negative forcing. It is beyond the scope of the present study to delve into these potential influences of the transported BC; however, the following paragraphs present initial estimates of just the direct radiative forcing of the BC in clear and cloudy skies.

[23] The direct radiative forcing due to the CFORS-predicted BC is estimated using the Monte Carlo Aerosol-Cloud-Radiation (MACR) model [*Podgorny et al.*, 2000; *Podgorny and Ramanathan*, 2001; *Vogelmann et al.*, 2001]. The BC profile applied in the MACR model simulation uses the CFORS model results above 1 km and assumes a well-mixed boundary layer of BC below 1 km as shown in Figure 14. The vertical BC distribution corresponds to the mean April 2004 BC concentration (as predicted by CFORS) spatially averaged over a rectangle bound by 35°N–60°N and 125°W–115°W. To calculate the forcing due to the BC, the radiation model is first run for a control case assuming purely scattering aerosol and then again after adding the CFORS BC in each atmospheric layer. Using a mass absorption efficiency of 10 m^2 g^{-1} [*Hansen*, 2003], the calculated AOD for the BC alone is 0.007. The background AOD for the scattering aerosol is obtained by subtracting the calculated BC AOD from the observed AOD of 0.124. The observed AOD is the mean April AOD measured at the Aerosol Robotic Network (AERONET) site [*Holben et al.*, 1998] located at Trinidad Head, CA (41.05°N, 124.15°W, 107 m). The atmospheric column single scattering albedo (SSA) was calculated by dividing the purely scattering AOD by the total (scattering plus absorbing) AOD and was equal to 0.944. This compares well to observed SSA values of 0.935 obtained at AERONET sites in this region.

[24] The calculated diurnal mean radiative forcing at top of the atmosphere (TOA), in the atmosphere, and at the surface is shown in Table 4. Under clear-sky conditions, the forcing attributed to the BC is larger at TOA and in the atmosphere over a land surface compared to the ocean; however, the surface dimming of −1.45 to −1.47 W/m^2

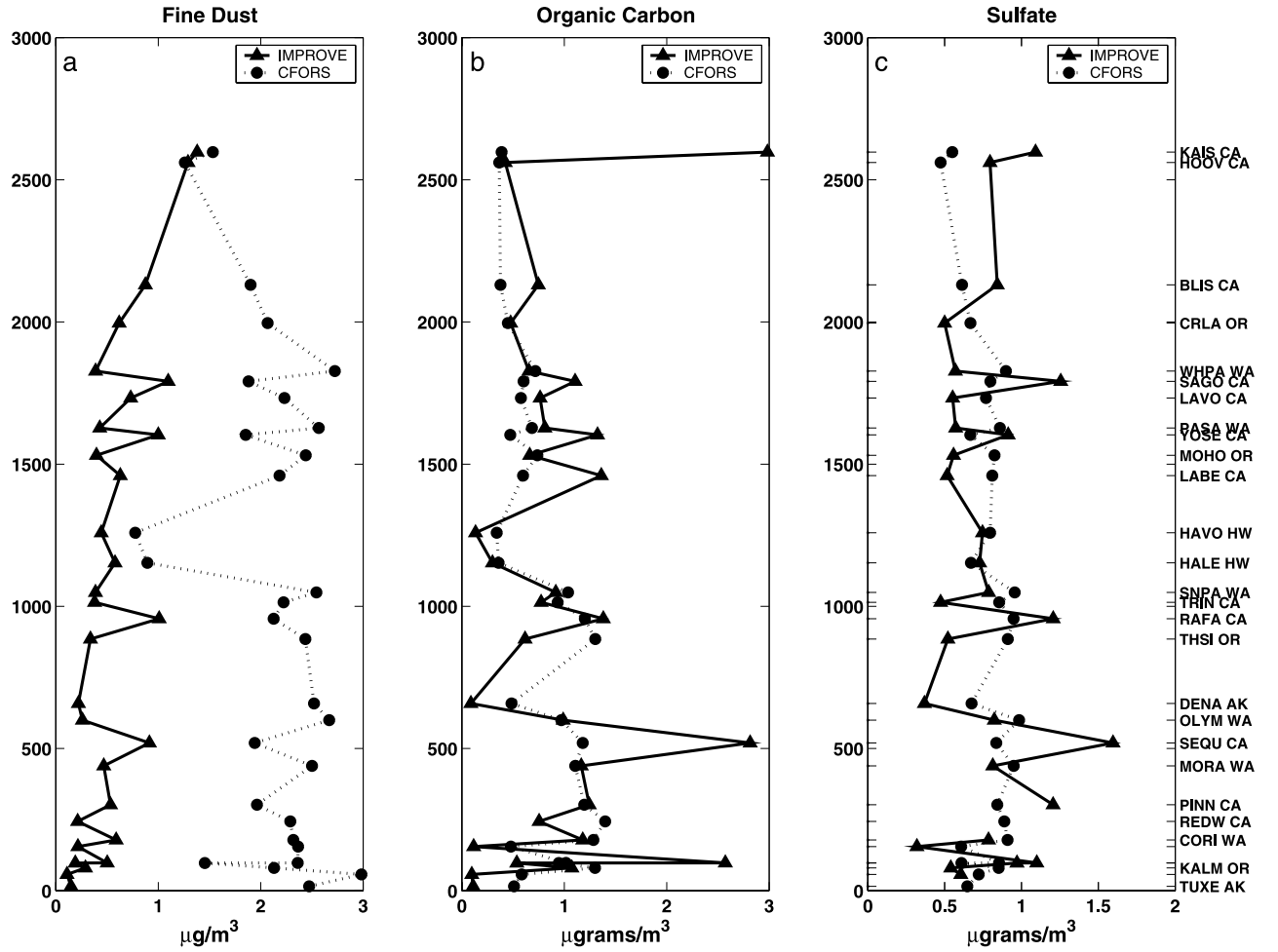

Figure 8. Comparison of IMPROVE and CFORS vertical distribution of (a) dust, (b) organic carbon, and (c) sulfate.

remains is approximately the same over both surfaces. This reduction in solar radiation at the surface could account for 20% of the 7 W/m^2 dimming over the United States reported by *Liepert and Tegen* [2002]. The positive forcing at TOA and in the atmosphere for both cases indicates an enhancement of the greenhouse effect, whereas a radiative cooling at the surface and a corresponding solar warming in the atmosphere suggest the possibility of changes in the tropospheric lapse rate.

[25] Inclusion of cloudy skies in the MACR model calculations decreases the magnitude of the overall forcing over both land and ocean. Relative to the clear-sky forcing, clouds reduce the negative surface forcing by 13% and the positive forcing in the atmosphere and at TOA by 27 and 61%, respectively (Table 4). These calculations, however, assume BC and cloud droplets as external mixtures. If BC is internally mixed with cloud droplets (e.g., by serving as nuclei), it can enhance aerosol solar absorption (by factors of 2–3) and therefore enhance the surface dimming. BC internally mixed with cloud drops or ice crystals has been shown to significantly enhance solar absorption [*Chylek and Hallett*, 1992; *Mikhailov et al.*, 2006]. The effects of enhanced absorption within clouds are discussed in several papers [*Chylek and Hallett*, 1992; *Chylek et al.*, 1984; *Conant et al.*, 2002; *Jacobson*, 2006; *Kaufman and Koren*, 2006]. Although a complex analysis of BC and cloud cover has not been conducted for this study, the MACR model results indicate that, to a first-order approximation, the BC and aerosol transport presented in this paper significantly impacts the radiation budget over both the Pacific Ocean and North America.

6. Conclusions

[26] In summary, this study points to a significant amount of Asian aerosol reaching North America during spring. Over 75% of the CFORS-modeled BC transport at 130°W originates in Asia, and this transport amounts to approximately 77% of the published estimates of North American BC emissions. This finding corroborates results from the ITCT 2K2 campaign, which found strong evidence for long-range transport of biomass burning and fossil fuel chemical indicators [*de Gouw et al.*, 2004], the two principal sources of BC. Ground-based measurements at Trinidad Head, CA, during ITCT 2K2 confirmed that Asian aerosols did reach the surface along the coast through downward mixing after passage of large frontal systems, but that on average, Asian pollution was concentrated at higher altitudes [*Heald et al.*, 2006] and impacted higher-elevation sites year-round [*VanCuren et al.*, 2005]. *Roberts et al.* [2006] observed that

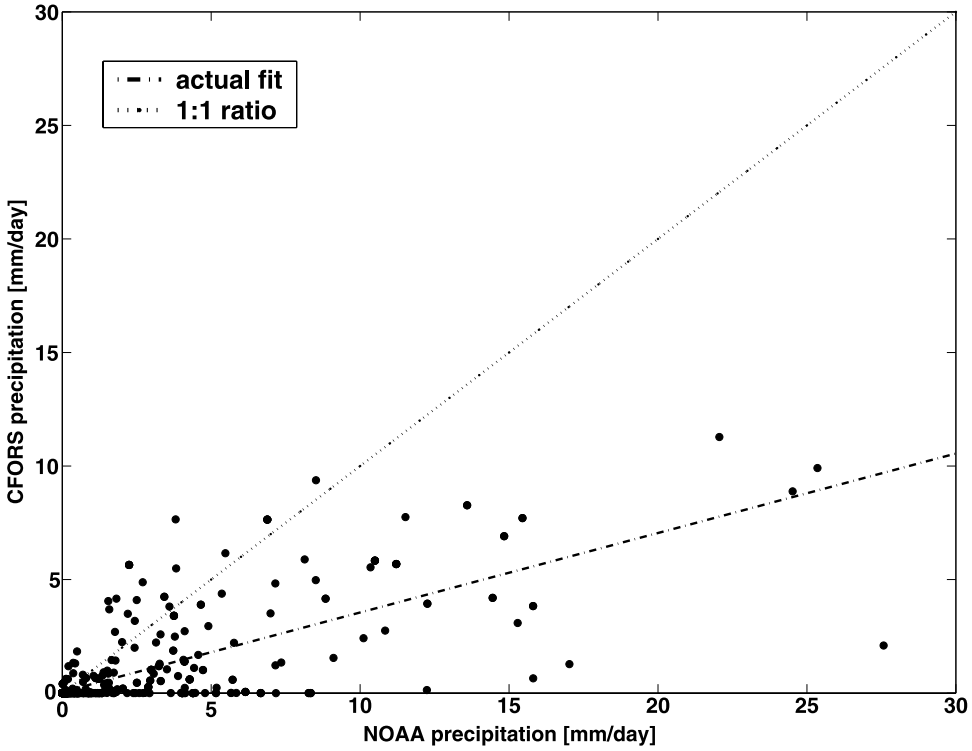

Figure 9. Scatterplot of CFORS precipitation vs. NOAA NCEP precipitation.

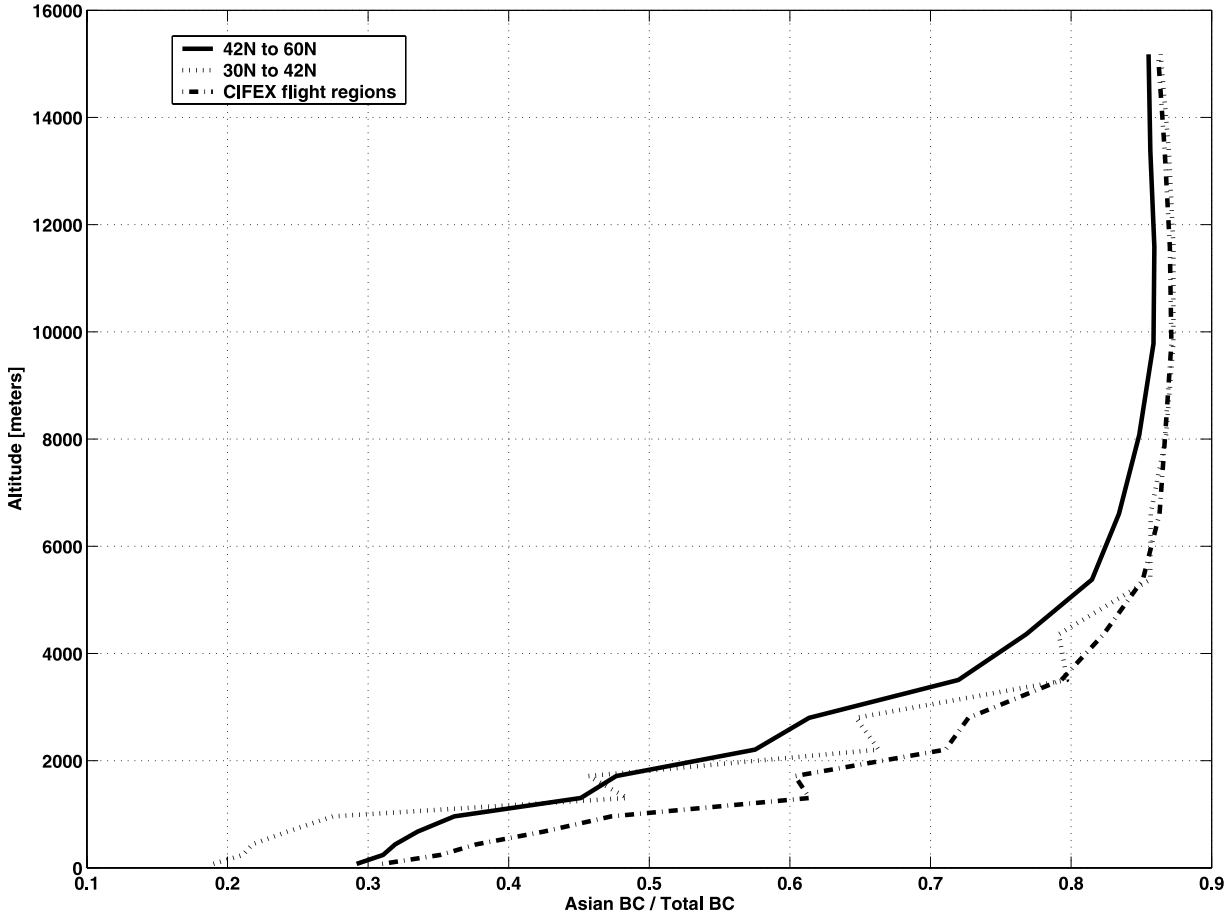

Figure 10. CFORS fraction of Asian BC to total BC as a function of altitude at 130°W.

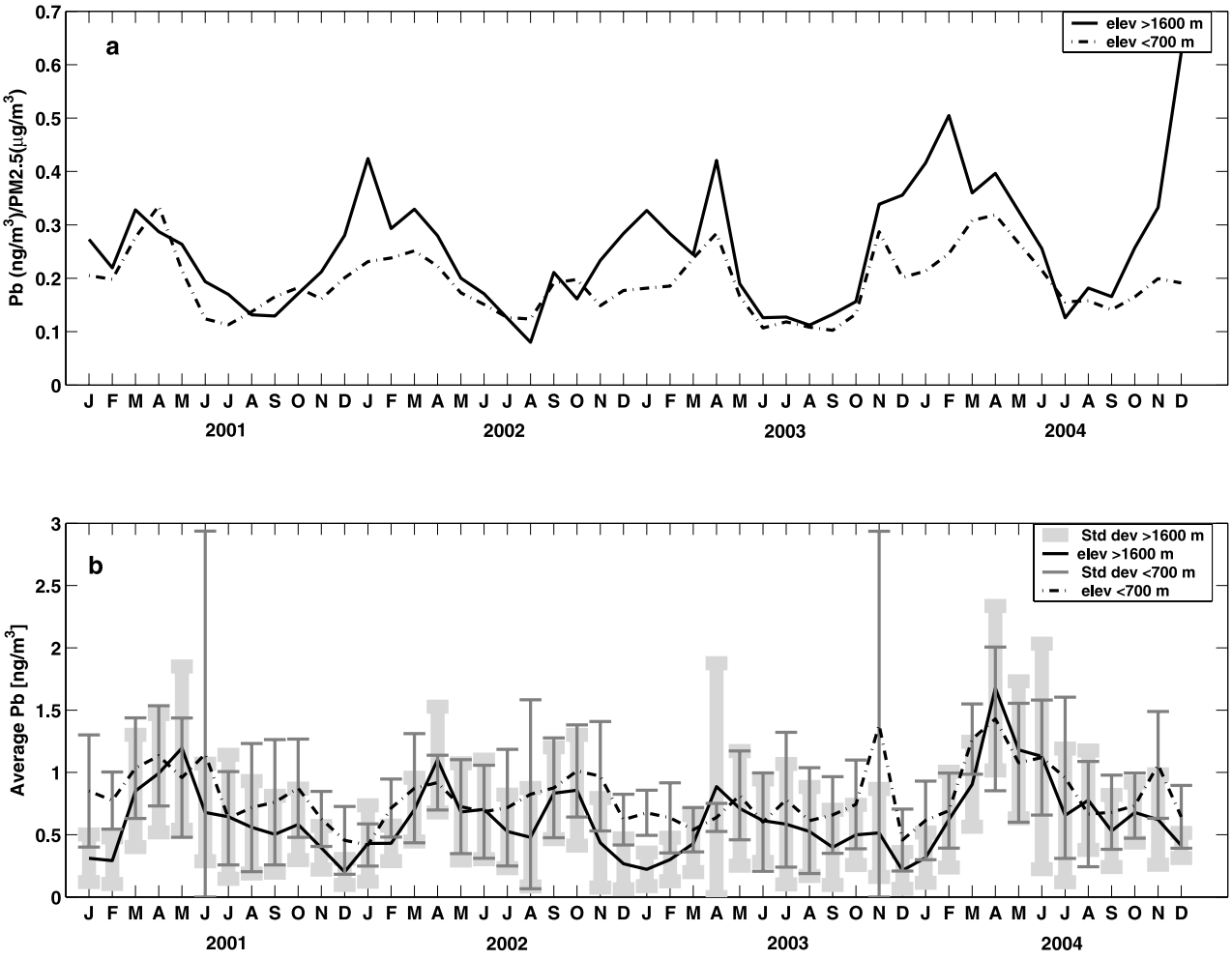

Figure 11. (a) Four-year time series of monthly averaged ratio of Pb to fine mass concentrations at high (>1600 m, solid line) and low (<700 m, dashed line) elevation IMPROVE sites in Washington, Oregon, and California; (b) a 4-year time series of the absolute monthly averaged Pb concentration at high- and low-elevation IMPROVE sites.

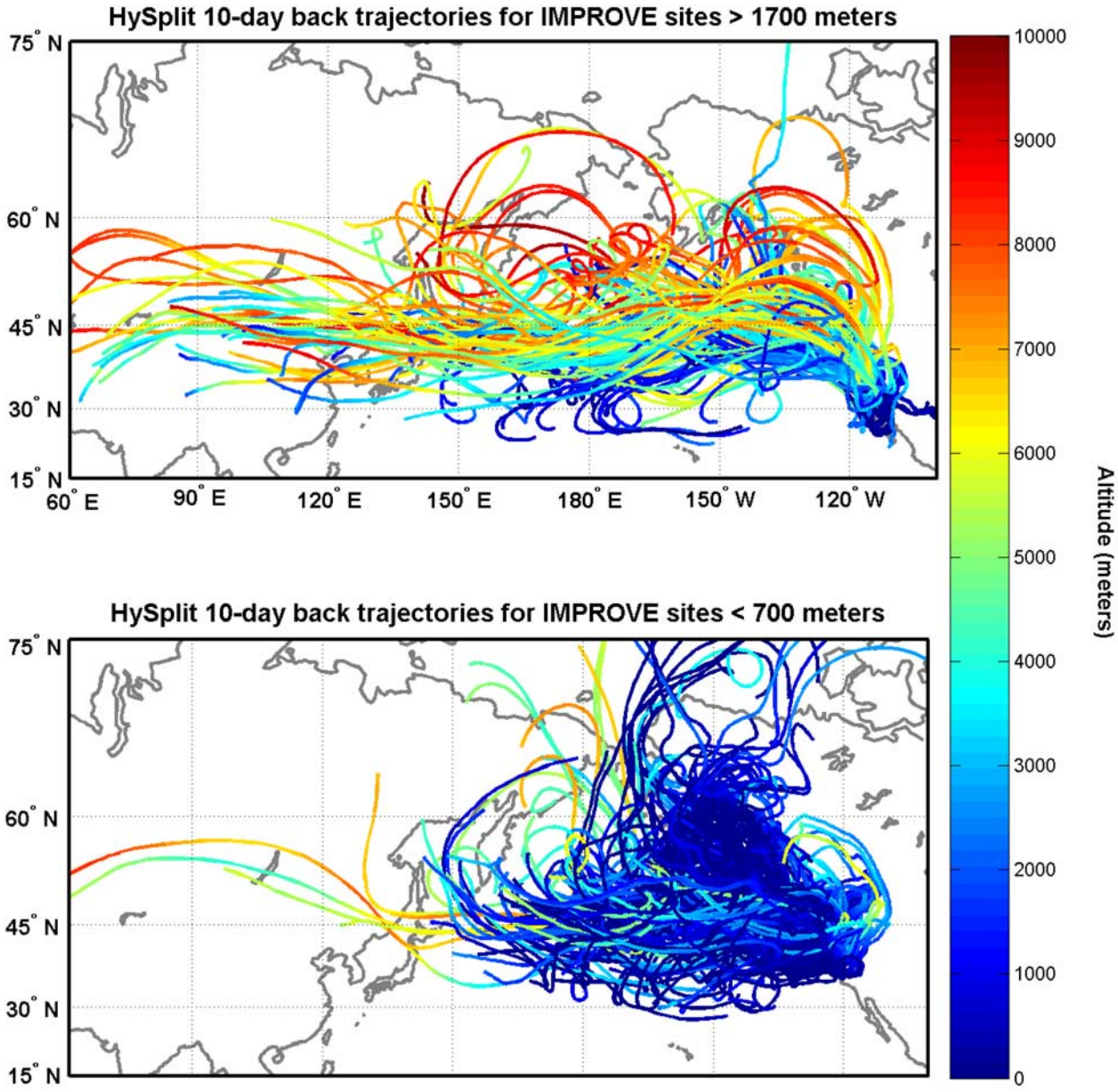

Figure 12. Ten-day, HYSPLIT back-trajectories at (a) high (>1700 m) elevation and (b) low (<700 m) elevation IMPROVE sites in California, Washington, and Oregon.

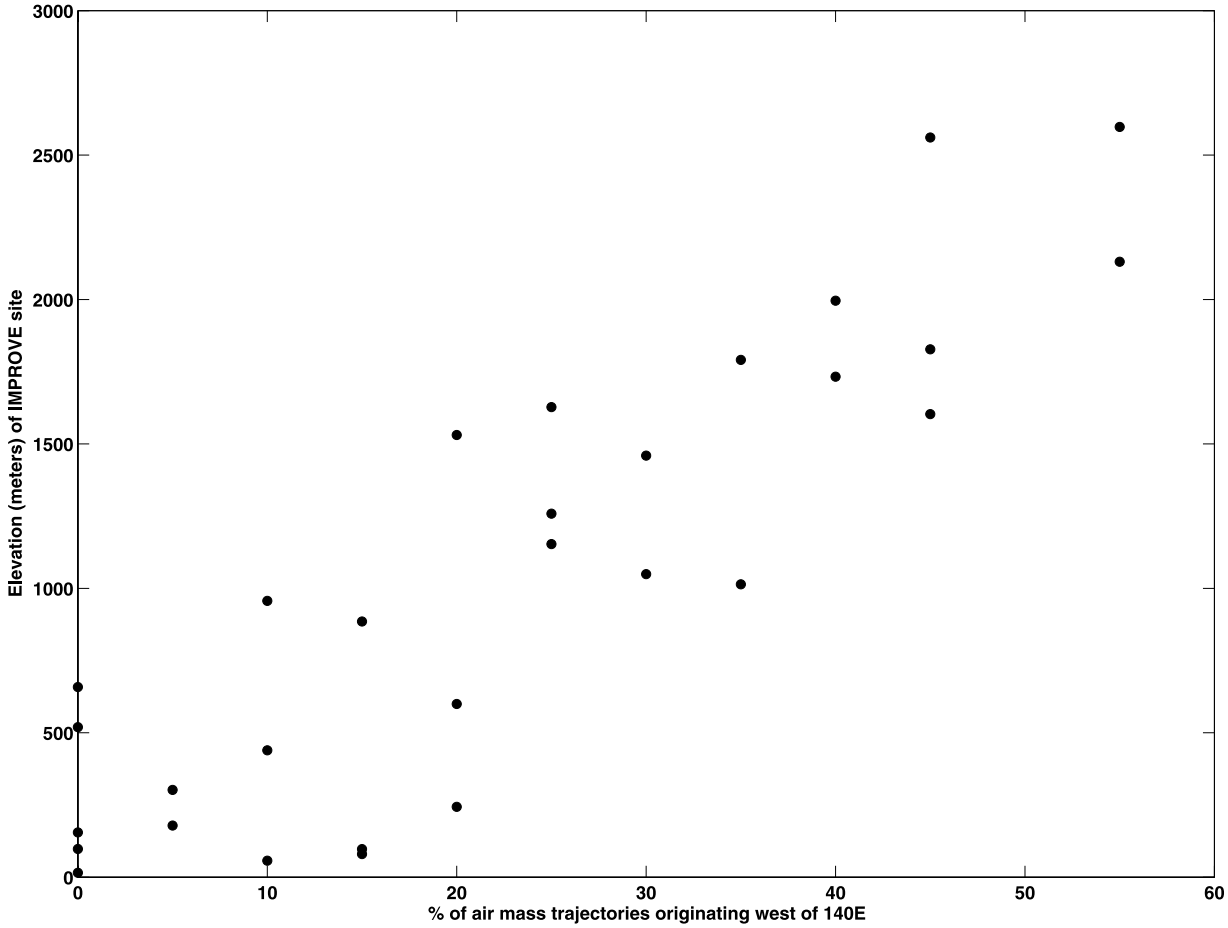

Figure 13. Scatterplot of IMPROVE elevation vs. percentage of air mass 10-day back-trajectories shown in Figure 12, with an endpoint west of 140°E.

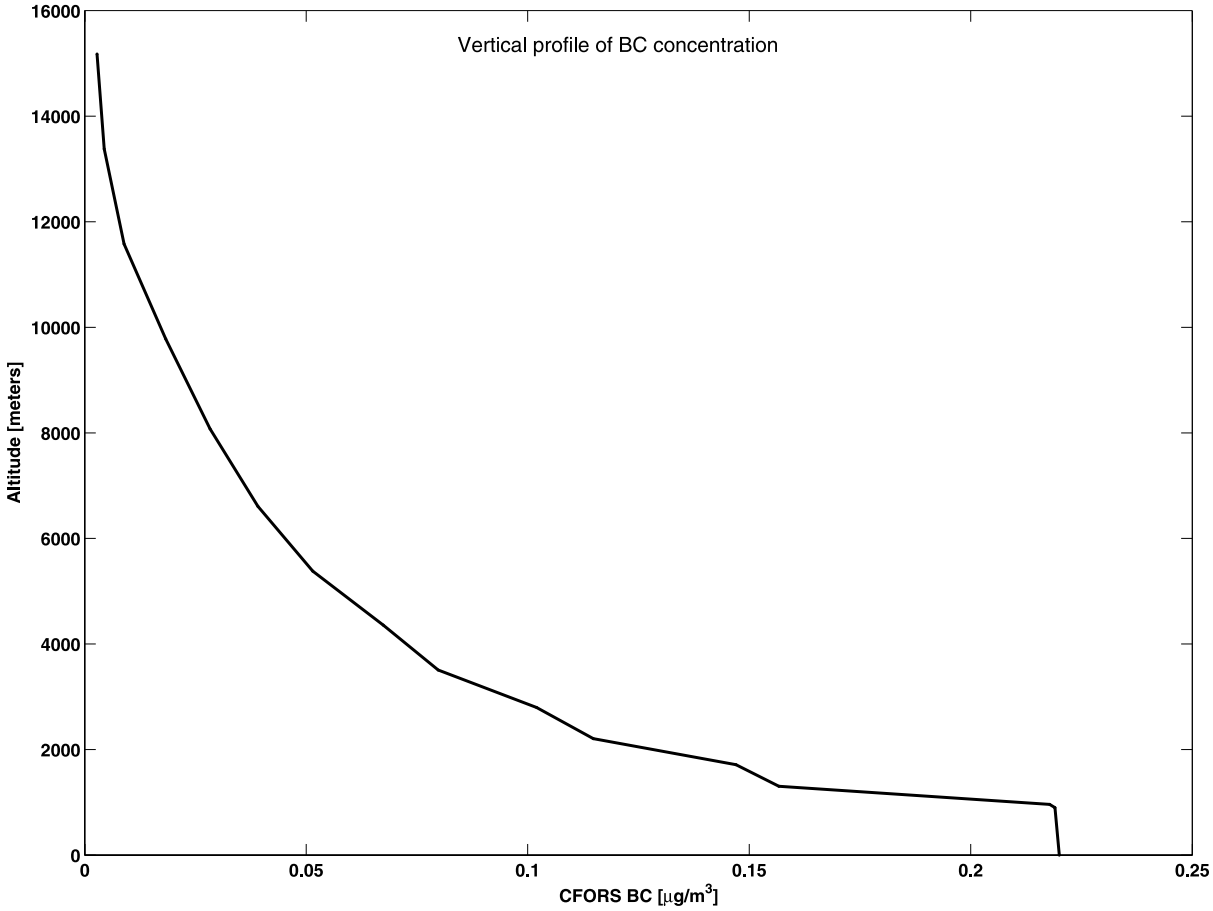

Figure 14. CFORS vertical profile of mean BC concentrations for April 2004, averaged over 30°N–60°N and 125°W–115°W. Below 1 km, a well-mixed boundary layer is assumed.

the aged aerosol, characteristic of long-range transport, appeared exclusively above 2500 m during the CIFEX flights. Comparison of CFORS to surface observations shows that the model accurately predicts concentration of BC, OC, and sulfate within 20% above 1 km. Flight data indicate that total fine mass is accurately simulated by CFORS above 2 and 6.5 km. Although the CFORS comparison with the IMPROVE dust data also shows agreement only above 2 km, the IMPROVE sites do not reach high enough to make a proper comparison with the flight data.

[27] On the basis of the comparisons of vertical profiles between the model and observations, we conclude that the CFORS-predicted transport for fine mass and BC above 2 km should be a reasonable approximation to the actual transport. The estimated fine aerosol and BC transports above 2 km for the month of April 2004 are 900 and 25 Gg, respectively. The corresponding transports for the entire atmosphere (surface to top of the atmosphere) are 1100 Gg (fine aerosol) and 32 Gg (BC). Thus the surface to 2-km region contributes only 22% to BC transport and 20% to fine aerosol mass transport, and the poor agreement with observed concentrations of BC and fine aerosol mass in the boundary layer should not overly impact the transport estimates. As a result, we recommend the range of 25–32 Gg for long-range BC transport and 900–1100 Gg for long-range fine aerosol transport into and above North America. This BC transport, which includes a significant fraction from Asia, may impact regional climate over both the western United States and the Pacific Ocean. The MACR model shows that the BC concentration predicted by CFORS over western North America absorbs an additional 2.04–2.55 W/m^2 in the atmosphere and causes a

Table 4. Radiative Forcing (in Wm^{-2}) due to the CFORS-Modeled BC and Calculated Using the MACR Model

	TOA	ATM	SFC	Comments
Ocean	0.59	2.04	−1.45	Clear-sky ocean (ocean diurnal mean albedo = 0.05)
	0.23	1.49	−1.26	Including regional mean cloud properties
Land	1.08	2.55	−1.47	Clear-sky land (land albedo = 0.23 from MODIS)
	0.66	1.91	−1.25	Including regional mean cloud properties

−1.45 to −1.47 W/m^2 dimming over land and ocean. Further implications of the transported BC and other Asian aerosol to regional radiation budget, cloudiness, and climate should be studied.

[28] **Acknowledgments.** We thank the National Science Foundation for funding CIFEX, NSF (ATM0201946), the National Oceanic and Atmospheric Administration (NA17RJ1231-VR03), and California Energy Commission (MR-06-01B) for their financial support of this study. We would also like to recognize the University of Wyoming, King Air crew, without whom much of the data could not have been collected, and all of the site operators of the IMPROVE monitoring network, as well as the analysis team at the Desert Research Institute for providing long-term measurements of aerosols at the IMPROVE aerosol observatories. Last, we would like to thank Dr. D. Kim for running the MACR simulations.

References

Abbatt, J., S. Benz, D. Cziczo, Z. Kanji, U. Lohmann, and O. Mohler (2006), Solid ammonium sulfate aerosols as ice nuclei: A pathway for cirrus cloud formation, *Science*, *313*, 1770.

Bertschi, I. T., and D. A. Jaffe (2005), Long-range transport of ozone, carbon monoxide, and aerosols to the NE Pacific troposphere during the summer of 2003: Observations of smoke plumes from Asian boreal fires, *J. Geophys. Res.*, *110*, D05303, doi:10.1029/2004JD005135.

Bey, I., D. J. Jacob, J. A. Logan, and R. M. Yantosca (2001), Asian chemical outflow to the Pacific in spring: Origins, pathways, and budgets, *J. Geophys. Res.*, *106*, 23,097–23,113.

Bond, T. C., D. G. Streets, K. F. Yarber, S. M. Nelson, J. H. Woo, and Z. Klimont (2004), A technology-based global inventory of black and organic carbon emissions from combustion, *J. Geophys. Res.*, *109*, D14203, doi:10.1029/2003JD003697.

Chow, J. C., J. G. Watson, L. W. A. Chen, W. P. Arnott, and H. Moosmuller (2004), Equivalence of elemental carbon by thermal/optical reflectance and transmittance with different temperature protocols, *Environ. Sci. Technol.*, *38*, 4414–4422.

Chylek, P., and J. Hallett (1992), Enhanced absorption of solar-radiation by cloud droplets containing soot particles in their surface, *Q. J. R. Meteorol. Soc.*, *118*, 167–172.

Chylek, P., V. Ramaswamy, and R. J. Cheng (1984), Effect of graphitic carbon on the albedo of clouds, *J. Atmos. Sci.*, *41*, 3076–3084.

Conant, W. C., A. Nenes, and J. H. Seinfeld (2002), Black carbon radiative heating effects on cloud microphysics and implications for the aerosol indirect effect—1. Extended Kohler theory, *J. Geophys. Res.*, *107*(D21), 4604, doi:10.1029/2002JD002094.

de Gouw, J. A., et al. (2004), Chemical composition of air masses transported from Asia to the U. S. West Coast during ITCT 2K2: Fossil fuel combustion versus biomass-burning signatures, *J. Geophys. Res.*, *109*, D23S20, doi:10.1029/2003JD004202.

Draxler, R. R., and G. D. Hess (1998), An overview of the HYSPLIT_4 modeling system for trajectories, dispersion, and deposition, *Aust. Meteorol. Mag.*, *47*, 295–308.

Eldred, R. A., and T. A. Cahill (1997), Sulfate sampling artifact from SO_2 and alkaline soil, *Environ. Sci. Technol.*, *31*, 1320–1324.

Eldred, R. A., T. A. Cahill, and R. G. Flocchini (1997), Composition of PM (2.5) and PM (10) aerosols in the IMPROVE network, *J. Air Waste Manage.*, *47*, 194–203.

Goldstein, A. H., et al. (2004), Impact of Asian emissions on observations at Trinidad Head, California, during ITCT 2K2, *J. Geophys. Res.*, *109*, D23S17, doi:10.1029/2003JD004406.

Hansen, A. D. A. (2003), *The Aethalometer*, Magee Scientific Company, Berkeley, CA.

Heald, C. L., D. J. Jacob, R. J. Park, B. Alexander, T. D. Fairlie, R. M. Yantosca, and D. A. Chu (2006), Transpacific transport of Asian anthropogenic aerosols and its impact on surface air quality in the United States, *J. Geophys. Res.*, *111*, D14310, doi:10.1029/2005JD006847.

Hendricks, J., B. Karcher, U. Lohmann, and M. Ponater (2005), Do aircraft black carbon emissions affect cirrus clouds on the global scale?, *Geophys. Res. Lett.*, *32*, L12814, doi:10.1029/2005GL022740.

Holben, B. N., et al. (1998), AERONET—A federated instrument network and data archive for aerosol characterization, *Remote Sens. Environ.*, *66*, 1–16.

Hsu, S. C., S. C. Liu, W. L. Jeng, F. J. Lin, Y. T. Huang, S. C. C. Lung, T. H. Liu, and J. Y. Tu (2005), Variations of Cd/Pb and Zn/Pb ratios in Taipei aerosols reflecting long-range transport or local pollution emissions, *Sci. Total Environ.*, *347*, 111–121.

Jacob, D. J., et al. (2003), Transport and chemical evolution over the Pacific (TRACE-P) aircraft mission: Design, execution, and first results, *J. Geophys. Res.*, *108*(D20), 9000, doi:10.1029/2002JD003276.

Jacobson, M. Z. (2006), Effects of externally-through-internally-mixed soot inclusions within clouds and precipitation on global climate, *J. Phys. Chem. A*, *110*, 6860–6873.

Jaffe, D., S. Tamura, and J. Harris (2005), Seasonal cycle and composition of background fine particles along the west coast of the US, *Atmos. Environ.*, *39*, 297–306.

Kaufman, Y. J., and I. Koren (2006), Smoke and pollution aerosol effect on cloud cover, *Science*, *313*, 655–658.

Liang, Q., L. Jaegle, D. A. Jaffe, P. Weiss-Penzias, A. Heckman, and J. A. Snow (2004), Long-range transport of Asian pollution to the northeast Pacific: Seasonal variations and transport pathways of carbon monoxide, *J. Geophys. Res.*, *109*, D23S07, doi:10.1029/2003JD004402.

Liepert, B., and I. Tegen (2002), Multidecadal solar radiation trends in the United States and Germany and direct tropospheric aerosol forcing, *J. Geophys. Res.*, *107*(D12), 4153, doi:10.1029/2001JD000760, 002002.

Liu, H. Y., D. J. Jacob, I. Bey, R. M. Yantosca, B. N. Duncan, and G. W. Sachse (2003), Transport pathways for Asian pollution outflow over the Pacific: Interannual and seasonal variations, *J. Geophys. Res.*, *108*(D20), 8786, doi:10.1029/2002JD003102.

Liu, Y. G., and P. H. Daum (2000), The effect of refractive index on size distributions and light scattering coefficients derived from optical particle counters, *J. Aerosol. Sci.*, *31*, 945–957.

Lohmann, U., B. Karcher, and J. Hendricks (2004), Sensitivity studies of cirrus clouds formed by heterogeneous freezing in the ECHAM GCM, *J. Geophys. Res.*, *109*, D16204, doi:10.1029/2003JD004443.

Mikhailov, E. F., S. S. Vlasenko, I. A. Podgorny, V. Ramanathan, and C. E. Corrigan (2006), Optical properties of soot-water drop agglomerates: An experimental study, *J. Geophys. Res.*, *111*(D7), D07209 doi:10.1029/2005JD006389.

Pacyna, J., and E. Pacyna (2001), An assessment of global and regional emissions of trace metals to the atmosphere from anthropogenic sources worldwide, *Environ. Rev.*, *9*, 269–298.

Park, R. J., et al. (2005), Export efficiency of black carbon aerosol in continental outflow: Global implications, *J. Geophys. Res.*, *110*, D11205, doi:10.1029/2004JD005432.

Parrish, D. D., Y. Kondo, O. R. Cooper, C. A. Brock, D. A. Jaffe, M. Trainer, T. Ogawa, G. Hubler, and F. C. Fehsenfeld (2004), Intercontinental Transport and Chemical Transformation 2002 (ITCT 2K2) and Pacific Exploration of Asian Continental Emission (PEACE) experiments: An overview of the 2002 winter and spring intensives, *J. Geophys. Res.*, *109*(D23), D23S01, doi:10.1029/2004JD004980.

Podgorny, I. A., and V. Ramanathan (2001), A modeling study of the direct effect of aerosols over the tropical Indian Ocean, *J. Geophys. Res.*, *106*, 24,097–24,105.

Podgorny, I. A., W. Conant, V. Ramanathan, and S. K. Satheesh (2000), Aerosol modulation of atmospheric and surface solar heating over the tropical Indian Ocean, *Tellus B*, *52*, 947–958.

Pruppacher, H. R., and J. D. Klett (1997), *Microphysics of Clouds and Precipitation*, 2nd ed., 954 pp., Springer, New York.

Ramanathan, V., B. R. Barkstrom, and E. F. Harrison (1989), Climate and the Earths Radiation Budget, *Phys. Today*, *42*, 22–32.

Roberts, G., G. Mauger, O. Hadley, and V. Ramanathan (2006), North American and Asian aerosols over the eastern Pacific Ocean and their role in regulating cloud condensation nuclei, *J. Geophys. Res.*, *111*, D13205, doi:10.1029/2005JD006661.

Sassen, K., P. J. DeMott, J. M. Prospero, and M. R. Poellot (2003), Saharan dust storms and indirect aerosol effects on clouds: CRYSTAL-FACE results, *Geophys. Res. Lett.*, *30*(12), 1633, doi:10.1029/2003GL017371.

Seinfeld, J. H., et al. (2004), ACE-ASIA—Regional climatic and atmospheric chemical effects of Asian dust and pollution, *Bull. Am. Meteorol. Soc.*, *85*, 367.

Stohl, A. (2001), A 1-year Lagrangian "climatology" of airstreams in the Northern Hemisphere troposphere and lowermost stratosphere, *J. Geophys. Res.*, *106*, 7263–7279.

Stolzenburg, M., N. Kreisberg, and S. Hering (1998), Atmospheric size distributions measured by differential mobility optical particle size spectrometry, *Aerosol. Sci. Technol.*, *29*, 402–418.

Streets, D. G., et al. (2003), An inventory of gaseous and primary aerosol emissions in Asia in the year 2000, *J. Geophys. Res.*, *108*(D21), 8809, doi:10.1029/2002JD003093.

Tanre, D., Y. J. Kaufman, M. Herman, and S. Mattoo (1997), Remote sensing of aerosol properties over oceans using the MODIS/EOS spectral radiances, *J. Geophys. Res.*, *102*, 16,971–16,988.

Uno, I., et al. (2003), Regional chemical weather forecasting system CFORS: Model descriptions and analysis of surface observations at Japanese island stations during the ACE-Asia experiment, *J. Geophys. Res.*, *108*(D23), 8668, doi:10.1029/2002JD002845.

VanCuren, R. A., and T. A. Cahill (2002), Asian aerosols in North America: Frequency and concentration of fine dust, *J. Geophys. Res.*, *107*(D24), 4804, doi:10.1029/2002JD002204.

VanCuren, R. A., S. S. Cliff, K. D. Perry, and M. Jimenez-Cruz (2005), Asian continental aerosol persistence above the marine boundary layer over the eastern North Pacific: Continuous aerosol measurements from Intercontinental Transport and Chemical Transformation 2002 (ITCT 2K2), *J. Geophys. Res.*, *110*, D09S90, doi:10.1029/2004JD004973.

Vogelmann, A. M., V. Ramanathan, and I. A. Podgorny (2001), Scale dependence of solar heating rates in convective cloud systems with implications to general circulation models, *J Clim.*, *14*, 1738–1752.

Wittmaack, K. (2002), Advanced evaluation of size-differential distributions of aerosol particles, *J. Aerosol. Sci.*, *33*, 1009–1025.

Yienger, J. J., M. Galanter, T. A. Holloway, M. J. Phadnis, S. K. Guttikunda, G. R. Carmichael, W. J. Moxim, and H. Levy (2000), The episodic nature of air pollution transport from Asia to North America, *J. Geophys. Res.*, *105*, 26,931–26,945.

Zheng, M., and M. Fang (2000), Correlations between organic and inorganic species in atmospheric aerosols, *Environ. Sci. Technol.*, *34*, 2721–2726.

G. R. Carmichael, Center for Global and Regional Environmental Research, University of Iowa, Iowa City, IA 52242, USA.

C. E. Corrigan, O. L. Hadley, G. S. Mauger, V. Ramanathan, and G. C. Roberts, Scripps Institution of Oceanography (SIO), Center for Atmospheric Sciences, University of California, 9500 Gilman Dr. #0239, San Diego, La Jolla, CA 92093, USA. (odelle@fiji.ucsd.edu)

Y. Tang, W/NP2, NOAA, WWB #207, 5200 Auth Road, Camp Springs, MD 20746-4304, USA.